Pyramidal neurons of upper cortical layers generated by NEX-positive progenitor cells in the subventricular zone

Sheng-Xi Wu*†, Sandra Goebbels‡, Kouichi Nakamura*, Kazuhiro Nakamura*, Kouhei Kometani§, Nagahiro Minato§, Takeshi Kaneko*¶, Klaus-Armin Nave‡, and Nobuaki Tamamaki*‖**

*Department of Morphological Brain Science and §Laboratory of Immunological Cell Biology, Graduate School of Medicine, Kyoto University, Kyoto 606-8501, Japan; †Department of Anatomy and K. K. Leung Brain Research Centre, Fourth Military Medical University, Xi'an 710032, People's Republic of China; ‡Department of Neurogenetics, Max Planck Institute of Experimental Medicine, D-37075 Goettingen, Germany; ¶Core Research for Evolutional Science and Technology (CREST) of Japan Science and Technology, Kawaguchi 332-0012, Japan; and ‖Department of Morphological Neural Science, Graduate School of Medical Sciences, Kumamoto University, Kumamoto 860-8556, Japan

Communicated by Richard L. Sidman, Harvard Medical School, Boston, MA, September 30, 2005 (received for review May 12, 2005)

The generation of pyramidal neurons in the mammalian neocortex has been attributed to proliferating progenitor cells within the ventricular zone (VZ). Recently, the subventricular zone (SVZ) has been recognized as a possible source of migratory neurons in brain slice preparations, but the relevance of these observations for the developing neocortex *in vivo* remains to be defined. Here, we demonstrate that a subset of progenitor cells within the SVZ of the mouse neocortex can be molecularly defined by Cre recombinase expression under control of the NEX/Math2 locus, a neuronal basic helix–loop–helix gene that by itself is dispensable for cortical development. NEX-positive progenitors are generated by VZ cells, move into the SVZ, and undergo multiple asymmetrical and symmetrical cell divisions that produce a fraction of the neurons in the upper cortical layers. Our data suggest that NEX-positive progenitors within the SVZ are committed to a glutamatergic neuronal fate and have evolved to expand the number of cortical output neurons that is characteristic for the mammalian forebrain.

glutamatergic | intermediate progenitor | neurogenesis | RCAS | neocortex

It is generally assumed that neurogenesis of the developing mammalian neocortex is restricted to the ventricular zone (VZ) (1–5), whereas the cell proliferation in the subventricular zone (SVZ) generates glial cells. Recently, Rakic and coworkers (6) suggested that in human embryonic tissue some SVZ cells generate neurons that can be immunostained for GABA. Also, in brain slices of the mouse maintained *in vitro*, single SVZ cells could be identified (by GFP labeling) that divided once symmetrically before giving rise to a pair of neocortical projection neurons (7). Other studies have shown that some progenitors within the SVZ divide once and generate cells expressing neuronal markers (8, 9). At later embryonic stages, the VZ is largely devoted to gliogenesis (10), suggesting that the generation of neurons for the cortical plate becomes compromised. At the outset of the present study, we hypothesized that (*i*) progenitors are maintained within the SVZ, where they persist as proliferating cells within a certain developmental window of cortical development, and that (*ii*) the generation of neocortical neurons in the SVZ compensates for the decline of neuronal progenitors within the late-embryonic VZ. However, the nature of these progenitors is purely hypothetical, and their presence *in vivo* has never been demonstrated. In the present study, we show that expression of a neuronal basic helix–loop–helix (bHLH) transcription factor gene, NEX, can be used as a molecular marker (11–13) to define a unique type of progenitor cell within the SVZ that differentiates into glutamatergic neurons. Using this marker, we can investigate early developmental features of glutamatergic neurons and their progenitors in the neocortex, both *in vivo* and *in vitro*.

Materials and Methods

Animals and Immunohistochemistry. All mouse embryos used in the present study were obtained by time-mating wild-type C57BL/6 mice or transgenic mice expressing GFP after Cre-mediated recombination (14) (Fig. 1*A*). For these breedings, we used homozygous mice harboring the Cre recombinase gene as a "knock-in" within the NEX locus (15). These mice are termed "NEX-Cre" and "NEX-GFP" mice, respectively (Fig. 1*A*). A neocortical area located medially about one third along the rostro-caudal axis was used for most of the following observations.

Immunohistochemistry was performed as described (4). Briefly, the embryos were perfused transcardially with saline, followed by 4% paraformaldehyde in phosphate buffer (pH 7.4). Fixed brains were removed, cryoprotected with 30% sucrose, and sectioned at a thickness of 20 μm. The following antibodies were used: rat anti-BrdUrd (Abcam; 1:1,000), rabbit anti-GFP (4) (0.5 μg/ml), mouse anti-Ki-67 (Pharmingen; 1:50), rabbit anti-P-H3 (Upstate Biotechnology; 1:1,000), rabbit anti-*tv-a* (gift of A. D. Leavitte; 1:300). Immunoreactive cells were revealed by biotinylated or fluorescent-dye-conjugated secondary antibodies and fluorescent-dye-conjugated streptavidin. Some sections were treated with propidium iodide (500 μM, Invitrogen). In brain sections of NEX-GFP mice, GFP was visualized by its fluorescence. Immuno- and GFP-fluorescence was observed with a confocal microscope (Pascal, Zeiss). For light microscopic observation, immunoreactive sites were visualized by diaminobenzidine (DAB) or NiDAB reaction.

Adenoviral and Retroviral Labeling of Neurons. An adenoviral construct was produced by inserting a cassette into the SwaI site of vector pAxcw (Takara, Tokyo), to obtain GFP expression after Cre-mediated recombination. This vector contained (from 5′ to 3′) cytomegalovirus enhancer, chicken actin (CA) promoter, loxP, chloramphenicol acetyltransferase gene, loxP, and GAP43 palmitoylation signal-GFP (ref. 4 and Fig. 1*A*). The adenovirus was produced by transfecting HEK 293 cells with the cosmid DNA according to the manufacturer's protocol. The titer of the resulting adenovirus supernatant was $\approx 6 \times 10^8$ plaque-forming units/ml.

An avian sarcoma and leukosis virus (ASLV) construct for GAP43 palmitoylation signal-GFP (GGFP) expression was generated by inserting a CMV promoter-GGFP cassette into the ClaI site of vector RCASBP(A) (16). The resulting plasmid was transfected

Conflict of interest statement: No conflicts declared.

Abbreviations: VZ, ventricular zone; SVZ, subventricular zone; bHLH, basic helix–loop–helix; ASLV, avian sarcoma and leukosis virus; E*n*, embryonic day *n*; IZ, intermediate zone; MZ marginal zone; Ara-C, arabinosylcytosine.

**To whom correspondence should be addressed. E-mail: tamamaki@medic.kumamoto-u.ac.jp.

© 2005 by The National Academy of Sciences of the USA

www.pnas.org/cgi/doi/10.1073/pnas.0508560102

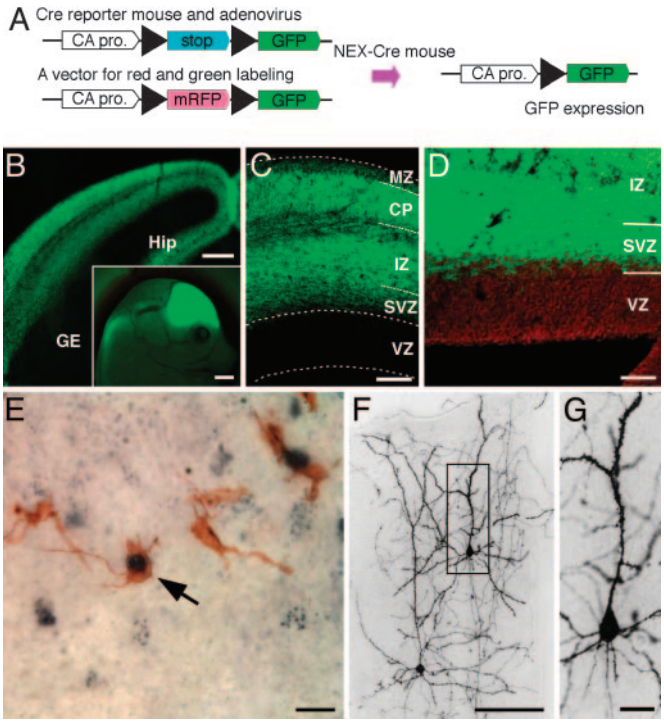

Fig. 1. Distribution of GFP-positive cells marked by NEX-Cre mediated cell lineage analysis. (*A*) Schematic diagram of cell lineage tracing using double-transgenic (NEX-GFP) mice. In NEX-positive cells, Cre recombinase removes a loxP-flanked stop sequence, bringing together the chicken actin (CA) promoter and the coding region for GFP. (*B*) Frontal section of the NEX-GFP mouse at E15. Subcortical regions, i.e., ganglionic eminence (GE), lack GFP staining (*Inset*, sagittal view of the E15 embryonic head). (*C*) Frontal section of the NEX-GFP neocortex at E15. Note that GFP-positive cells are absent from the VZ and MZ. (*D*) A clear boundary emerges between VZ and SVZ after counterstaining with propidium iodide. (*E–G*) One day after injection of recombinant adenovirus into the lateral ventricle of NEX-Cre embryos (E14), a number of cells in the SVZ are immunostained for both GFP (brown) and P-H3 (dark blue) (arrow in *E*). Three weeks after injection, basically all NEX-GFP-marked cells developed into pyramidal neurons in the upper cortical layers (*E*). At higher magnification, NEX-GFP-marked cells (boxed in *E*) reveal spiny processes (*F*). (Scale bars: 1 mm in *B Inset*; 200 μm in *B*; 100 μm in *C* and *F*; 50 μm in *D*; and 20 μm in *E* and *G*.) Sections in *B–D* are 20 μm, and those in *E–G* are 50 μm in thickness.

into CEF cells by calcium phosphate precipitation. Supernatant was collected 48 h after transfection, centrifuged at low speed to remove cell debris, aliquoted, and stored at −80°C until use. The titer of the dissolved ASLV solution was 1×10^6 pfu/ml. After the injection of virus, transduced cells were visualized by GFP-immunohistochemistry. To visualize proliferating Cre-positive cells, we introduced a TVA expression vector as a Cre reporter into VZ cells at embryonic day 15 (E15). The *tv-a* 800 vector [CA promoter–loxP–CAT–loxP–*tv-a*-poly(A); see Fig. 1*A*] was introduced by *in vivo* electroporation (15 V; 50-ms duration; 5 Hz for 1 s; Tokiwa, Tokyo), after the injection of recombinant virus into the lateral ventricle of the embryonic brain.

Immunocytochemistry and Single-Cell PCR. Brains were derived from E15 NEX-GFP-mouse embryos and cut into 200-μm-thick coronal sections by using a microslicer (Dosaka EM, Kyoto). Under a fluorescence microscope, neocortical slices were divided into upper halves [from the intermediate zone (IZ) to the marginal zone (MZ)] and lower halves (from the VZ to the IZ), and the latter was treated with trypsin-EDTA (0.1% in PBS, pH 7.4) and dissociated into single cells by gentle pipetting. Dissociated cells were spread onto gelatin-coated glass slides and stained by double-immunofluorescence for GFP/P-H3 and GFP/Ki-67. For single-cell RT-PCR, the dissociated cells were dispersed onto 6-cm dishes containing culture medium. Individual GFP-positive cells were viewed, aspirated, and transferred into the RT-PCR solution (Quixell, Stoelting, Wood Dale, IL). For single-cell RT-PCR, we used M-MLV reverse transcriptase (Invitrogen) and HotStarTaq DNA polymerase (Qiagen). The presence of *Svet1* and Ki-67 in single NEX-GFP positive cell was examined by nested PCR. As a standard, β-actin cDNA was also amplified by RT-PCR in each sample. The primers used in this study are as follows: for detection of *Svet1* mRNA, 5′-GGC ACC ATT ACA ACA CCA CACC-3′, 5′-GTC CTTT GTG CTG TCC CCA TTT-3′, 5′-GCC TGT GAG TGG AAA AGA ATGG-3′, 5′-TGA TGT CAC CAG GGG AAG ATGT-3′; for detection of Ki-67 mRNA, 5′-CAA CAT TAC AAA GCA AAA GCA-3′, 5′-GCT TAG GTT CAC TGT CCA AA-3′, 5′-CAC CAA AGC AGG AAG CAA CA-3′, 5′-TTG GCC CCG AGA TGT AGA TT-3′; for detection of β-actin mRNA, 5′-GCC AAC CGT GAA AAG ATG AC-3′, 5′-GCA CTG TGT TGG CAT AGA GG-3′, 5′-GGC TGT GCT GTC CCT GTA TG-3′, 5′-CAA GAA GGA AGG CTG GAA AA-3′.

Fluorescence-Activated Cell Sorting and Immunoblotting. Neocortex was dissected from NEX-GFP-mouse embryos at E15 and dissociated into single cells as described above. GFP-positive cells were sorted by using a FACS Vantage (Becton Dickinson). Sorted cells (1×10^6 cells) were resuspended and cultured in Neurobasal medium (GIBCO) that was conditioned with embryonic brain tissue overnight, containing 5% B27 supplement (GIBCO), 20 ng/ml basic FGF, 20 ng/ml EGF, and 5 μg/ml BrdUrd, in the presence or absence of arabinosylcytosine (Ara-C) (0.5 μM). After 2-day culture, cells were lysed and their DNA was extracted. Five nanograms of DNA was used for immunoblotting and detected with a rat anti-BrdUrd antibody and an ECL kit (Amersham Pharmacia).

Transplantation. Pregnant NEX-GFP mice were given a single i.p. injection of BrdUrd (50 mg per kg of body weight) at E15. Embryos were harvested after 30 min, and their brains were removed immediately. Frontal sections (200 μm) were prepared from the middle third of the embryonic telencephalon, and the dissociation of cells from the upper half of the neocortex (Fig. 2 *I* and *J*) was performed as described above. After centrifugation, the dissociated cells were transplanted into the neocortex of wild-type mice at postnatal day 0, using a microsyringe (22–26 gauges per inch) inserted along the surface of the neocortex. One week later, mice were killed and their brains were fixed and processed for immunohistochemistry. Serial sections were immunostained by using anti-GFP and anti-BrdUrd antibodies.

Results

When sections were taken from the cortex of mice at E13 and cells were stained at the M phase with immunohistochemistry of a cell cycle marker, the phosphorylated histone H3 (P-H3), ≈25% of all mitotic cells (259 of 1,028) were located within the SVZ. By E15, this fraction increased to 33.3% (364 of 1,093), and many mitotic cells could be seen in the IZ, possibly derived from the SVZ (Fig. 5, which is published as supporting information on the PNAS web site). This proliferative activity in the SVZ coincides with the generation of pyramidal neurons destined for the upper cortical layers (17). Therefore, we searched for a molecular marker of SVZ cells (at E15), when many mitotic and P-H3 immunoreactive cells are present. One such marker is the bHLH transcription factor NEX, widely expressed in mature neocortical and hippocampal pyramidal neurons, as well as in immature cells of the SVZ and the cortical plate in the embryonic cortex (11–13).

We used NEX-Cre mice that were created as a knock-in of the Cre gene into the NEX locus (S.G. and K.-A.N., unpublished data) and mated them with a strain of conditional GFP-expressing mice

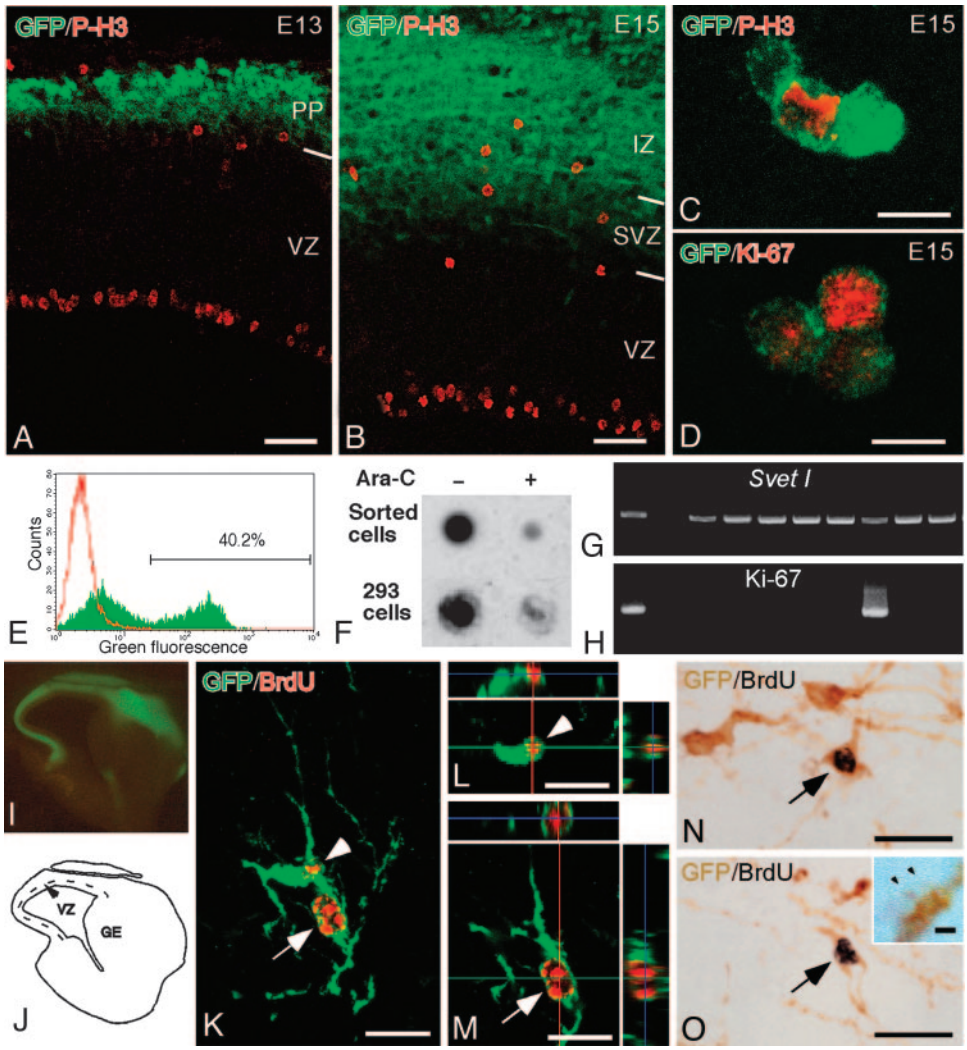

Fig. 2. Proliferative activity of NEX-GFP-marked cells in the SVZ. (*A* and *B*) P-H3 immunoreactive cells in the neocortex of NEX-GFP mouse embryos at E13 (*A*) and E15 (*B*). P-H3-positive cells at the ventricular edge are radial glia in mitosis. In addition P-H3-positive cells were found in the outer part of the VZ, the SVZ, and the IZ. Most of the P-H3-positive cells in the SVZ and the IZ are positive for GFP at E15, whereas they were negative for GFP at E13. PP, preplate. (*C* and *D*) NEX-GFP-marked dissociated cells (green) with P-H3 immunoreactivity (red in *C*), or with Ki-67 immunoreactivity (red in *D*), obtained from the neocortex of NEX-GFP embryos at E15. (*E*) FACS profile of dissociated cells. Green, NEX-GFP-marked cells; red, wild-type controls. The GFP-marked cells (40.2% of the dissociated cells) were collected and maintained in culture. (*F*) Dot blot analysis for the detection of BrdUrd in genomic DNA of sorted cells. DNA was purified from the sorted cells (in *E*) and from HEK293 control cells after 2-day culture in a medium containing BrdUrd, with or without antimitotic drug (Ara-C). Note that sorted GFP-positive cells, similar to HEK 293 cells, incorporate BrdUrd in the absence of Ara-C. (*G* and *H*) Single-cell RT-PCR and detection of Svet1 (*G*) and Ki-67 (*H*) transcripts in GFP-expressing SVZ cells, dissociated from NEX-GFP mouse embryos (E15). Most of the GFP-marked cells (9 of 10) were positive for Svet1, and 2 of 10 GFP-positive cells were positive for Ki-67. (*I* and *J*) Microphotograph (*I*) and schematic depiction (*J*) of the neocortex, appearing like a flat cap without VZ and SVZ, microdissected from a NEX-GFP mouse embryo at E15. BrdUrd was administered to pregnant NEX-GFP mice i.p. Thirty minutes later, the embryonic brains were removed and the neocortex was dissected as shown (in *J*) and dissociated into single cells. The dissociated cells were transplanted into the neocortex of the newborn mice and recovered 1 week later. (*K*) Confocal image of a pair of GFP: (green) and BrdUrd (red) double-labeled cells. (*L* and *M*) Three-dimensional view to confirm GFP expression by two BrdUrd-labeled cells (same as shown in *K*), marked with arrow and arrowhead, respectively. (*N* and *O*) Pair of two spiny neurons (arrows) immunostained for GFP (brown) and BrdUrd (black) on adjacent sections (*O Inset*, spines of double-labeled spiny neurons at higher magnification. Arrowheads indicate the spine heads). (Scale bars: 50 μm in *A* and *B*, 10 μm in *C* and *D*, 20 μm in *K*–*O*, and 1 μm in *O Inset*.) Sections in *A*, *B*, and *K*–*M* are 20 μm, and those in *N* and *O* are 50 μm in thickness.

(14). Cre expression was regulated properly in the NEX locus and overlapped well with NEX expression (13). Because homozygous NEX-Cre (knock-out) mice show no developmental defect, also heterozygous mutants and their offspring develop normally, with all cells in the NEX-lineage being GFP-labeled. At E15, GFP expression marked the entire neocortex, limbic cortex, olfactory bulb, and olfactory cortex, from the SVZ to the cortical plate, but not the VZ and the MZ (Fig. 1 *A*–*C*).

Because of the high cellular density in the developing cortex, the morphology of individual GFP-labeled neurons was difficult to discern, even at high magnification. Therefore, we marked individual NEX-Cre expressing cells by prior transduction with a recombinant adenovirus at E14, harboring a conditional (flox-stopped) GFP reporter gene. One day after the virus was injected into the lateral ventricle of NEX-Cre mice, we noted that the vast majority of GFP-positive recombinant cells were multipolar in shape and located within the SVZ (Fig. 1*D*). Three weeks after birth, all GFP-positive cells had the morphological characteristics of spiny neurons in the upper cortical layers (Fig. 1 *E* and *F*). Importantly, we did not observe GFP-labeled astrocytes or other nonneuronal

cells, nor any GFP-labeled aspiny or sparsely spiny neurons. In fact, 95% of all GFP-positive cells (932 of 981) were identified as pyramidal neurons in the upper cortical layers, as judged by the presence of typical apical dendrites. The remaining 5% of GFP-positive cells (49 of 981) exhibited spiny dendrites but lacked a visible apical dendrite, most likely because of the plane of section. This finding strongly suggested that the GFP-positive multipolar cells, virally marked in the SVZ at E15, are the progenitors of mature GFP-positive pyramidal neurons. Judging from the time point of their appearance in the SVZ, these GFP-positive multipolar cells are daughter cells of stem cells or progenitors in the VZ (4, 18).

Interestingly, when we immunolabeled GFP-positive cells for P-H3 as a mitotic marker (1 day after adenovirus infection), we found a significant number of double-positive cells (13 of 298, 4.3%) in the SVZ (Fig. 1*D*). Thus, at least some of the NEX-Cre marked multipolar cells in the SVZ are mitotic progenitors that might correspond to the intermediate progenitors that produce pairs of neocortical projection neurons *in vitro* (7). It is perhaps interesting to compare these intermediate progenitors that maintain processes and appear multipolar during mitosis, to radial glial cells that maintain long radial processes during mitosis (3–5).

Moreover, the distribution of GFP-positive cells overlapped with the distribution of P-H3-stained cells in the SVZ at E15, but not at E13 (Fig. 2 *A* and *B*). P-H3 positive SVZ cells at E13 may correspond to the intermediate progenitors that express neurogenin-2 (9). This finding suggested that committed precursors of pyramidal neurons can be marked by NEX-lineage tracing. To confirm overlapping expression at the cellular level, we microdissected the deeper halves of the neocortex (from the VZ to the IZ), dissociated the pieces of tissue into single cells, and mounted them onto glass slides for coimmunostaining of GFP and P-H3, or GFP and Ki-67. Among all NEX-GFP-positive cells (the majority of which represent postmitotic neurons), a small but significant fraction of 1.2% (16 of 1,334) still expressed P-H3 (Fig. 2*C*), and 14.3% (31 of 286) were positive for the proliferation antigen Ki-67 (Fig. 2*D*). Similarly, when dissociated NEX-GFP-positive cells were sorted by FACS and cultured in a medium containing BrdUrd, they incorporated the nucleotide analogue into nuclear DNA (Fig. 2 *E* and *F*). Incorporation of BrdUrd was prevented by addition of the antimitotic drug cytosine-β-D-arabinofuranoside (Ara-C). Finally, we performed single cell RT-PCR analyses of dissociated cells from the microdissected lower half of the neocortex. Here, the majority of NEX-GFP-expressing cells (43 of 48 or 89.6%) also expressed *Svet1*, a neuronal marker of upper neocortical layers (19) (Fig. 2*G*). Among these double-positive cells, a significant fraction (4 of 24 or 16.7%,) also expressed Ki-67 (Fig. 2*H*). Taken together, these data demonstrate that a sizeable fraction of NEX-GFP-marked cells in the SVZ of E15 embryos are progenitors that have not yet exited the cell cycle, although they are committed to become upper layer pyramidal neurons (also referred to as "intermediate progenitors" below).

Transplantation experiments demonstrated that intermediate progenitors also exist outside the SVZ (see Fig. 5) and are committed to become pyramidal neurons. NEX-Cre mice were mated with the conditional GFP expressing Cre reporter mice, and 30 min after i.p. BrdUrd injection of pregnant females (at E15), brains of double-transgenic embryos were removed. The upper halves of the neocortex (from the IZ to the MZ, including cells that have migrated away from the SVZ) were microdissected and dissociated into individual cells (Fig. 2 *I* and *J*). NEX-GFP-positive cells were transplanted into host brains of wild-type mice at birth. Seven days after transplantation, all GFP-positive cells derived from the transplant showed spiny dendrites (Fig. 2 *K–O*). Moreover, most GFP and BrdUrd double-labeled cells had a thick and long apical dendrite bearing spines and several short spiny dendrites originating from the soma (Fig. 2 *K–O* and *O Inset*). Some of these cells were readily identifiable as pyramidal neurons (Fig. 2*N*), and most (16 of 22 or 72.7%) were found in pairs. The occurrence of pairs of BrdUrd-positive pyramidal neurons is most likely due to a terminal cell division of the intermediate progenitors of neocortical projection neurons (7).

In neocortical development, generating the correct number of pyramidal neurons depends critically on the number of mitotic cycles of their progenitors (2). To investigate how many times a mitotic cell that was generated in the VZ and has moved into the SVZ divides as a secondary progenitor, we followed two lines of experiments.

First, by using explant cultures and video microscopy, we tried to directly observe the proliferation of single NEX-Cre-positive cells. To this end, we used a plasmid containing two reporter genes that can be "switched" by Cre recombination from expressing a red fluorescent protein (mRFP) to expressing GFP (see *Supporting Text*, which is published as supporting information on the PNAS web site). These plasmids were introduced (by electroporation) into VZ cells of NEX-Cre mouse embryos, and the emergence and behavior of fluorescent cells was observed in *ex vivo* preparations. Successfully electroporated VZ cells were revealed by the red fluorescence, and NEX-Cre-positive daughter cells (originating from the VZ) were revealed by green fluorescence (see right side of Movie 1, which is published as supporting information on the PNAS web site). Importantly, we observed not only symmetrical cell divisions (7), but also stationary NEX-GFP-positive cells undergoing asymmetrical divisions with only one small daughter cell migrating away from field of view. The small daughter cells were produced by budding of spherical protrusion (Movies 1–3, which are published as supporting information on the PNAS web site).

In the second line of experiments, we used the ASLV system, in which only proliferating cells that also express ASLV receptor (TVA) can be successfully transduced with a retrovirus (16). Two vectors were simultaneously injected into the lateral ventricle of NEX-Cre mice: (*i*) a plasmid for the conditional (Cre-mediated) expression of the ASLV receptor protein in transfected cells, and (*ii*) a recombinant ASL retrovirus for GFP expression in successfully transduced cells (Fig. 3*A*). After the delivery of retroviral particles and plasmid DNA into the brain, the syringe needle was connected to an electrical pulse generator and used *in situ* as a negative electrode for electroporation (Fig. 3*A*). By passing a current from the positive electrode (on the surface of the brain) to the syringe needle, the plasmid DNA was transfected into cells located along a narrow area of the neocortical VZ (Fig. 3 *A–C*). When the syringe needle was retracted, the surface of the VZ was slightly scratched which allowed retroviral particles to invade the intercellular space of the VZ and to reach the SVZ. Thus, any NEX-Cre-positive cell in the SVZ that had taken up the conditional *tv-a* 800 expression plasmid at an earlier stage (i.e., by electroporation in the VZ) became TVA-positive (Fig. 3 *B* and *C*). If such a cell was still mitotic, it could be successfully transduced (by ASLV) and permanently marked by GFP expression as a progenitor cell of pyramidal neurons. In a pilot experiment, we introduced the ASLV and the plasmid DNA for TVA expression into the embryonic brains by injection and electroporation, but made no scratch into the VZ. In 20 embryonic brains obtained from this series, we found no single GFP-positive cell. This finding demonstrates that ASLV does not transduce TVA-negative cells, and that electroporation does not help ASLV to infect TVA-negative cells.

The reported cell cycle duration in the SVZ is 15 h (20). Because ASLV is a simple retrovirus (16), proviral integration occurs in one of both daughter cells generated in the previous cell cycle. Thus, if intermediate progenitors would proliferate continuously, we calculated that for one infection, maximally two cells are GFP-labeled within 2 days (or four to eight cells within 3 days, etc.). If intermediate progenitors divide only once, the maximum number of GFP-positive cells in a clonal cell cluster is one, even after 3 days.

Mouse brains that were electroporated and virally infected at E15, were analyzed 2–10 days later. Thirty mouse embryos were

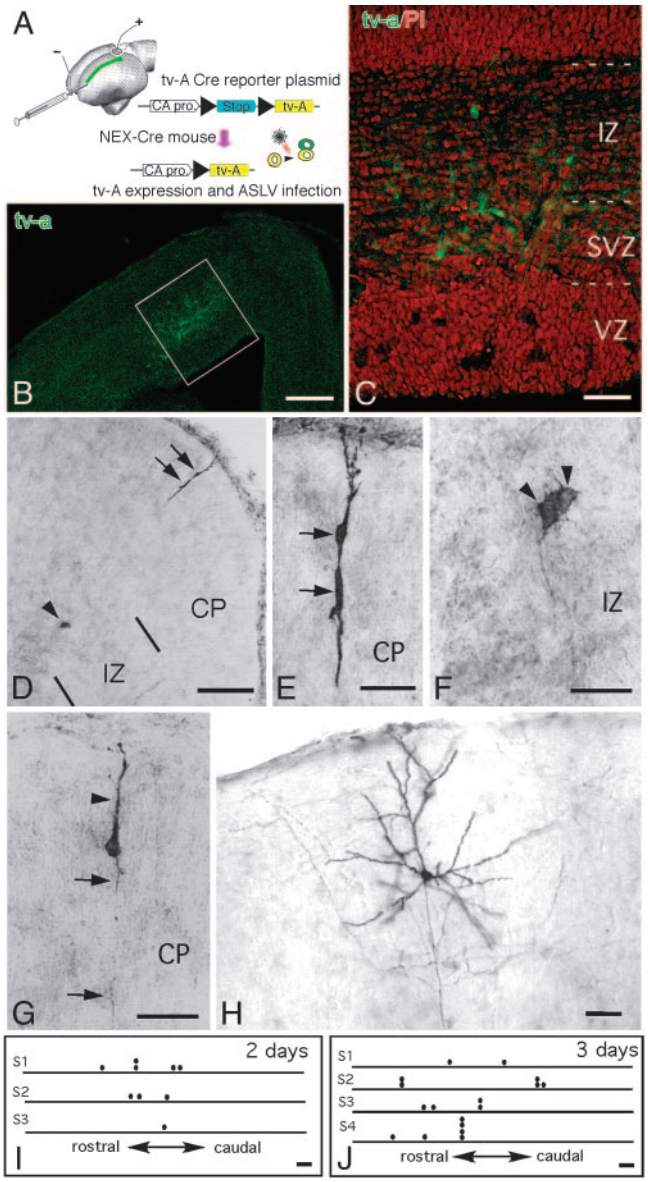

Fig. 3. NEX-Cre-mediated lineage analysis after ASLV infection. (*A*) Schematic depiction of the microinjection and electroporation procedures used for introducing both *tv-a*-expression vector and ASLV retrovirus into the lateral ventricle of E14 NEX-Cre mice. The tv-a 800 expression vector expresses TVA upon recombination by Cre. The position of TVA marked cells is indicated (in green). (*B*) Distribution of TVA-positive cells (green) in the neocortex one day after transduction. (*C*) Higher magnification of the framed area (in *B*) reveals individual TVA-positive cells in the SVZ and IZ. Propidium iodide (red) is used for counterstaining. (*D–F*) Example of a clone that has been detected by anti-GFP staining 3 days after retrovirus injection. Depicted in *E* and *F* are higher magnifications of the GFP-positive cells shown in *D*. (*G* and *H*) Labeled immature and mature pyramidal neurons 3 and 10 days after injection, respectively. (*I* and *J*) Schematic representation of neuronal clones in different brain samples (S1–S4). Each horizontal bar indicates the rostral-to-caudal dimension of a brain, with circle dots symbolizing the position of GFP-positive cells. (Scale bars: 200 μm in *B*; 50 μm in *C*; 100 μm in *D*, *I*, and *J*; and 25 μm in *E–H*.)

fixed and processed for TVA immunohistochemistry. Fourteen embryos successfully expressed TVA at the dorsal part of the neocortex and were analyzed for the distribution of GFP-labeled cells, either 2 or 3 days after virus injection. Three embryos were delivered normally, and one mouse was used for analysis. Because the ASLV receptor (TVA) was expressed in a narrow rostro-caudal

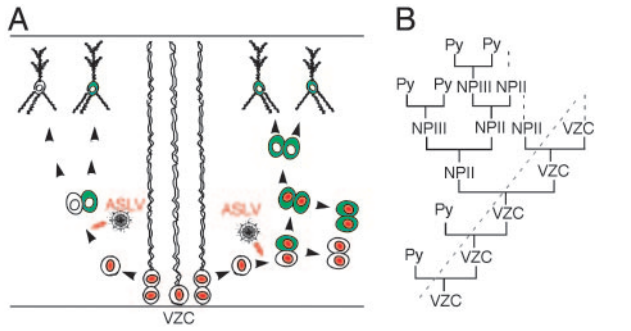

Fig. 4. Model for the generation of pyramidal neurons in the SVZ. (*A*) Depending on the infected cells, single pyramidal neuron or four-cell clusters are revealed by ASLV infection (green) after 3 days. Red cell nuclei indicate proliferative activity. Note that the ASLV reporter virus transduces only TVA expressing mitotic cells (NEX-Cre positive progenitors). (*B*) Presumed lineage relationship of VZ cells (VZC), the secondary neuronal progenitors (NPII), tertiary neuronal progenitors (NPIII), and pyramidal neuron (Py). A dotted line marks the boundary between VZ and SVZ.

band (Fig. 3*A*), in agreement with previous reports describing a radial alignment of clonally related neocortical neurons (3, 21–24), almost all GFP-labeled cells were restricted to this narrow band (Fig. 3 *B* and *C*). Although other studies have shown viral labeling of clones that became widely distributed over the cortex (25, 26), we did not encounter GFP-labeled cells that were distributed outside of this TVA-positive narrow band in 3 days.

Two days after virus injection, we counted three pairs of cells and three GFP-labeled solitary cells in three embryonic brains (another four brains failed to show GFP labeling). At 3 days after virus injection, we found one four-cell cluster, one three-cell cluster, three pairs of cells, and four solitary cells (Fig. 3 *D–J*) in four brains, and three other brains showing no GFP labeling. All clusters were separated from individually labeled cells by a distance of several hundred μm in the rostro-caudal direction. If all 26 GFP-positive cells were labeled by infection of individual cells (along the rostro-caudal linear scratch made in 14 embryonic brains), the chance of finding repeatedly the clustered cellular distribution that is shown in Fig. 3 *I* and *J* would be very small ($P < 0.01$). Thus, we assume that single ASLV infections have labeled more than two cells, most likely by secondary proliferation. If ASLV infected cells were already "clustered" along the scratch, one should recognize these clusters as groups of GFP-positive cells within 1 day after infection. Instead, two-cell clusters were only observed 2 days after ASLV infection (or later), and three- and four-cell clusters were only observed 3 days after ASLV infection (or later). Thus, it is unlikely that labeled clusters of cells reflect merely "clusters" of viral infection. Becaus ASLV is replication-incompetent in mammalian cells (16), we consider each GFP-labeled-cell cluster as a clone that started from a single NEX-Cre-positive progenitor. In good agreement with our theoretical prediction, we counted a maximum of two labeled cells in one cluster after 2 days, and maximally four cells in one cluster after 3 days (Fig. 3 *D–F*). This finding indicated that some NEX-Cre-positive intermediate progenitors are proliferating continuously during the observational period, whereas others divide only once or twice. A single GFP-positive cell develops into an immature pyramidal neuron within 3 days (Fig. 3*E*). Within 10 days, a solitary GFP-positive neuron of the upper neocortical layer has extended apical dendrites and axon branches, participating in the neocortical circuitry (Fig. 3*H*).

Discussion

In this study, we have used Cre recombinase, experimentally coexpressed with a neuron-specific bHLH gene (NEX/Math2), as

a molecular marker that allows us to identify neuronal progenitor cells *in vivo* that proliferate outside the VZ. The GFP-labeling of mature pyramidal neurons by NEX-Cre lineage marking (after adenoviral infection) as well as the transplantation study of NEX-GFP-marked cells demonstrate independently that neuronal progenitor cells reside in the SVZ and are committed to become spiny excitatory neurons of the neocortex. We currently do not know whether NEX-Cre-positive cells include all proliferative neuronal progenitors or only a subset. However, the progenitors observed in this study behaved differently from those reported previously (7–9), most notably by revealing both symmetric and asymmetric cell divisions. We also demonstrated the proliferation of progenitor cells directly by time lapse video microscopy.

The application of ASLV conditional transduction in this study allowed us to trace the behavior of individual progenitor cells *in vivo* and to follow their final fate. Depending on the type of progenitor cell transduced by ASLV, different numbers of GFP-labeled progeny were revealed. A solitary cell is most likely the result of retroviral infection of one progenitor before its terminal cell division (Fig. 4*A Left*). A four-cell cluster, composed of a pair of multipolar cells in the intermediate zone and a pair of bipolar cells in the cortical plate (Fig. 3 *D–F*), would be predicted for the retroviral infection of one progenitor cell dividing three more times in 3 days (Fig. 4*A Right*). Depending on the mixed morphology of the products in 3 days (multipolar and bipolar cells), one can assume that some cell divisions in this clone have been asymmetric.

Based on these *in vivo* and *in vitro* studies, we propose a model by which the generation of cortical pyramidal neurons is not restricted to the VZ and involves both symmetric and asymmetric cell divisions outside the VZ (Fig. 4*B*). According to this model, VZ cells (regarded as the primary neuronal progenitors or NPI) divide to produce intermediate progenitor cells (7–9). Some intermediate progenitors proliferated several times, thereby expanding the pool of secondary neuronal progenitors (NPII). Other intermediate progenitors, which we designated as the ''tertiary'' neuronal progenitors (NPIII), are generated by asymmetric cell division of NPII, and undergo their final symmetrical division to produce two pyramidal neurons each (7). Whereas most proliferating cells in the VZ are multipotential stem cells, NEX-expressing intermediate progenitors appear committed to become glutamatergic neurons, and thus provide a source of projection neurons during corticogenesis. These intermediate progenitors are derived from radial glia and differentiated further in the lineage of glutamatergic neocortical neurons. A similar concept of primary and secondary (and tertiary) neuronal progenitors is well accepted for cerebellar and hippocampal development. In these brain regions, the proliferative cells are more clearly (also spatially) separated from the VZ, and have thus been recognized a long time ago (27). The shift of neurogenesis from the VZ to the SVZ in the embryonic neocortex may be related to the emergence of adult neurogenesis in the SVZ (28).

The expression of several proneuronal bHLH genes has been associated with neurogenesis in the VZ (29), whereas the specification of neuronal cell fate does not require the expression of the NEX gene itself (11–13). Rather, NEX is a differentiation factor, functionally related to neuroD and NDRF (13), that emerges as a marker of neuronal cell fate. It is possible that many more committed neuronal progenitors coexist in the SVZ and that they simply do not express the NEX gene at this stage. In mice, NEX-positive intermediate progenitors may play a minor role for the final number of neocortical neurons. However, secondary progenitors hold the potential to significantly expand the neocortex by simply adding mitotic cycles. In primates, the neocortex has a dramatically increased volume and surface, associated with the convoluted growth of the cortical plate, whereas the VZ remains flat. The secondary amplification of neuronal progenitor cells that we describe here may be a mechanism underlying the neocortical expansion in primate evolution (30).

We thank A. D. Leavitt (University of California, San Francisco), C. L. Cepko (Harvard Medical School, Boston), S. H. Hughes (National Cancer Institute, Frederick, MD), and R. Tsien (Stanford University, Stanford, CA) for providing us with antibodies and vectors. This study was supported by a Grant-in-Aid for Scientific Research on Priority Area-Advanced Brain Science Project from the Ministry of Education, Culture, Sports, Science and Technology, Japan, the Bundesministerium für Bildung und Forschung, and the Deutsche Forschungsgemeinschaft.

1. Angevine, J. B. & Sidman, R. L. (1961) *Nature* **192,** 766–768.
2. Takahashi, T., Nowakowski, R. S. & Caviness, V. S., Jr. (1995) *J. Neurosci.* **15,** 6046–6057.
3. Noctor, S. C., Flint, A. C., Weissman, T. A., Dammerman, R. S. & Kriegstein, A. R. (2001) *Nature* **409**, 714–720.
4. Tamamaki, N., Nakamura, K., Okamoto, K. & Kaneko, T. (2001) *Neurosci. Res.* **41,** 51–60.
5. Miyata, T., Kawaguchi, A., Okano, H. & Ogawa, M. (2001) *Neuron* **31,** 727–741.
6. Letinic, K., Zoncu, R. & Rakic, P. (2002) *Nature* **417,** 645–649.
7. Noctor, S. C., Martinez-Cerdeno, V., Ivic, L. & Kreigstein, A. R. (2004) *Nat. Neurosci.* **7,** 136–144.
8. Haubensak, W., Attardo, A., Denk, W. & Huttner, W. B. (2004) *Proc. Natl. Acad. Sci. USA* **101,** 3196–3201.
9. Miyata, T., Kawaguchi, A., Saito, K., Kawano, M., Muto, T. & Ogawa, M. (2004) *Development (Cambridge, U.K.)* **131,** 3133–3145.
10. Voigt, T. (1989) *J. Comp. Neurol.* **289,** 74–88.
11. Bartholoma, A. & Nave, K. A. (1994) *Mech. Dev.* **48,** 217–228.
12. Shimizu, C., Akazawa, C., Nakanishi, S. & Kageyama, R. (1995) *Eur. J. Biochem.* **229,** 239–248.
13. Schwab, M. H., Bartholomae, A., Heimrich, B., Feldmeyer, D., Druffel-Augustin, S., Goebbels, S., Naya, F. J., Zhao, S., Frotscher, M., Tsai, M. J., *et al.* (1998) *J. Neurosci.* **18,** 1408–1418.
14. Novak, A., Guo, C., Yang, W., Nagy, A. & Lobe, C. G. (2000) *Genesis* **28,** 147–155.
15. Schwab, M. H., Bartholomae, A., Heimrich, B., Feldmeyer, D., Druffel-Augustin, S., Goebbels, S., Naya, F. J., Zhao, S., Frotscher, M., Tsai, M. J., *et al.* (2000) *J. Neurosci.* **20,** 3714–3724.
16. Hughes, S. H., Greenhouse, J. J., Petropoulos, C. J. & Sutrave, P. (1987) *J. Virol.* **61,** 3004–3012.
17. Takahashi, T., Goto, T., Miyama, S., Nowakowski, R. S. & Caviness, V. S., Jr. (1999) *J. Neurosci.* **19,** 10357–10371.
18. Hashimoto, M. & Mikoshiba, K. (2004) *J. Neurosci.* **24,** 286–296.
19. Tarabykin, V., Stoykova, A., Usman, N. & Gruss, P. (2001) *Development (Cambridge, U.K.)* **128,** 1983–1993.
20. Takahashi, T., Nowakowski, R. S. & Caviness, V. S., Jr. (1995) *J. Neurosci.* **15,** 6058–6068.
21. Walsh, C. & Cepko, C. L. (1988) *Science* **241,** 1342–1345.
22. Kornack, D. R. & Rakic, P. (1995) *Neuron* **15,** 311–321.
23. Rakic, P. (1995) *Proc. Natl. Acad. Sci. USA* **92,** 11323–11327.
24. Soriano, E., Dumesnil, N., Auladell, C., Cohen-Tannoudji, C. & Sotelo, C. (1995) *Proc. Natl. Acad. Sci. USA* **92,** 11676–11680.
25. Walsh, C. & Cepko, C. L. (1992) *Science* **255,** 434–440.
26. Walsh, C. & Cepko, C. L. (1993) *Nature* **362,** 632–635.
27. Hatten, M. E. & Heintz, N. (1999) *Neurogenesis and Migration: Fundamental Neuroscience*, eds. Zigmond, M. J., Roberts, J. L., Bloom, F. E. & Spitzer, N. C. (Academic, San Diego), pp. 451–479.
28. Deotsch, F., Caille, I., Lim, D. A., Garcia-Verdugo, J. M. & Alvarez-Buyllar, A. (1999) *Cell* **97,** 703–716.
29. Ross, S. E., Greenberg, M. E. & Stiles, C. D. (2003) *Neuron* **39,** 13–25.
30. Smart, I. H. M., Dehay, C., Giroud, P., Berland, M. & Kennedy, H. (2002) *Cereb. Cortex* **12,** 37–53.